Computationally Exploring Confinement Effects in the Methane-to-Methanol Conversion Over Iron-Oxo Centers in Zeolites

Florian Göltl,[*,†,‡] Carine Michel,[‡] Prokopis C. Andrikopoulos,[‡] Alyssa M. Love,[†] Jürgen Hafner,[¶] Ive Hermans,[*,†,§] and Philippe Sautet[*,‡,‖]

†*University of Wisconsin - Madison, Department of Chemistry, University Avenue 1101, 53706 Madison, Wisconsin, USA*

‡*Univ Lyon, Ens de Lyon, CNRS UMR 5182, Universit Claude Bernard Lyon 1, Laboratoire de Chimie, F69342, Lyon, France*

¶*University of Vienna, Faculty of Physics, Computational Materials Physics, Sensengasse 8/12, 1090 Vienna, Austria*

§*University of Wisconsin - Madison, Department of Chemical and Biological Engineering, 1415 Engineering Drive, 53706 Madison, Wisconsin, USA*

‖*Department of Chemical and Biomolecular Engineering, University of California Los Angeles, Los Angeles, CA 90005, United States*

E-mail: fgoeltl@wisc.edu; hermans@chem.wisc.edu; sautet@ucla.edu

Abstract

Transitionmetal-oxo centers in zeolites are known to be active in the conversion of methane to methanol. Here we study this reaction over Fe-oxo sites in the zeolite SSZ-13. By comparing calculations for the fully periodic structure and a cluster for two different methods, the standard van der Waals corrected semi-local density functional PBE-D2 and ACFDT-RPA, a method where correlation is calculated fully non-locally, we find that it is actually the confining environment in the zeolite that reduces the barrier for this reaction by more than 50 % and that the two applied methods lead to qualitatively different results.

Keywords: confinement effects, methane, methanol, zeolites, density functional theory, ACFDT-RPA

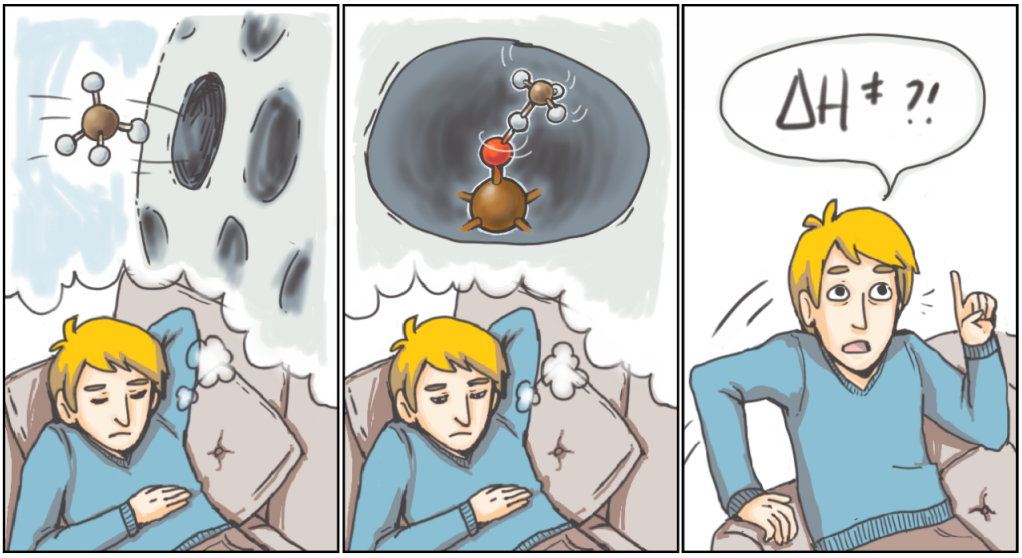

The direct conversion of methane to methanol at low temperatures using oxygen is one of the long standing challenges in catalysis. Several methods have been suggested, but many of the catalysts known today are prone to over oxidation and formation of CO_2.[1] However, in nature methane monooxygenase enzymes are able to catalyze this reaction at room temperature[2–4] and the nature of the active sites has acted as inspiration for the design of similar heterogeneous catalysts. Particularly promising systems in this context are Cu-[5–8] and Fe-

exchanged zeolites,[9,10] which show activity for the formation of methoxy species bound to the active sites at low temperature. Critical steps when applying these catalysts are the creation and regeneration of the active sites and the extraction of methanol. Most of the experiments have been performed in a stepwise procedure, where first the active site is created under high O_2 pressures at elevated temperatures, then methane is activated at lower temperatures and finally methanol is extracted by introducing water.[7] Only most recently a fully catalytic process using O_2 to regenerate the active sites has been reported.[11] Interestingly, Cu- and Fe-sites in different zeolite structures are able to catalyze this reaction at low temperatures,[5–10] while similar active sites in other materials lead to less favorable properties. Therefore it is a natural assumption that not only the structure and stoichiometry, but also the confining environment of the active sites plays a critical role.

Confinement effects in zeolite catalysis have been studied in the context of a variety of reactions, such as alkane activation,[13,14] the conversion of methanol to dimethyl ether[15] or the conversion of biomass.[16,17] Early ideas about these confinement effects include (i) diffusional restrictions for molecules accessing the active sites, (ii) geometric constraints for transition states and (iii) diffusional restrictions for products.[18–20] While all these phenomena qualitatively explain an increase in selectivity, they are not able to quantitatively capture the influence of confinement on the reaction rate. Based on ideas about separating activation energies into contributions from the molecular adsorption process, and to the catalytic reaction itself,[21,22] research has more recently focused on quantifying the impact of confinement by separating entropy and enthalpy contributions to the two components.[14,23] As Gounder and Iglesia pointed out,[14] due to the temperature dependence of the Gibbs Free Energy, the effect of confinement on activation enthalpies will be dominant at the low temperatures encountered in the conversion of methane to methanol. While it is possible to measure apparent reaction barriers experimentally, theory is a key tool to provide an atomistic understanding of each reaction step. However, the accurate description of chemical and non-local interactions between reactant molecules and the zeolite lattice is still challenging for most commonly

used density functionals[24] and they have been shown to lead to qualitatively wrong results for the deprotonation of tert-butyl cations in protonated zeolites.[25]

In this work we study the impact of different levels of electronic structure theory on the description of the conversion of methane to methanol over Fe-oxo centers in zeolites. We focus on two different methods, PBE-D2[26,27] and the Adiabatic-Connection Fluctuation-Dissipation Theorem in its Random-Phase Approximation (RPA).[28] While the former is a widely used standard semi-local Generalized Gradient Approximation functional with empirical dispersion corrections, the latter one is a high-level electronic structure method with a non-local treatment of correlation. Both methods have successfully been applied to model the adsorption of short alkanes in zeolites.[24] By understanding the similarities and differences between them, we find that confinement lowers the activation energy for this reaction by more than 50% and that the application of RPA as a high-level theory leads to qualitatively different results from most commonly used methods.

For the zeolite support we choose SSZ-13, which serves as a model system in understanding zeolite catalysis. It is a zeolite in the chabazite structure, which has the smallest primitive unit cell, and therefore allows the application of high-level methods in fully periodic calculations at a reasonable cost.[24] In this unit cell the Fe-oxo group is located in the six ring of the structure , where two Si atoms are substituted by Al on the opposite sides of the ring as displayed on the left hand side of Fig. 2, an active site similar to the ones suggested in Fe-exchanged Ferrierite.[29] Careful tests reveal that this site is most stable in the quintet spin state (see supporting information Fig. S1). As suggested for other zeolites[30] and the metal organic framework Fe-MOF-74,[31] this spin state does not change along the reaction pathway.

Two possible pathways have been suggested for the conversion of methane-to-methanol, namely the rebound mechanism[32,33] and a concerted mechanism.[34] As displayed in Scheme 1, the rebound mechanism is a two-step process where initially one H-atom is abstracted from CH_4, before the C-O bond is formed, while the concerted mechanism only contains one

reaction step and transition state. As we were not able to find a possible concerted path, in agreement with other reports in the literature,[30] we focus on the rebound mechanism. All the structural details are given in Fig. 1 and we will only briefly discuss the most important features in the text.

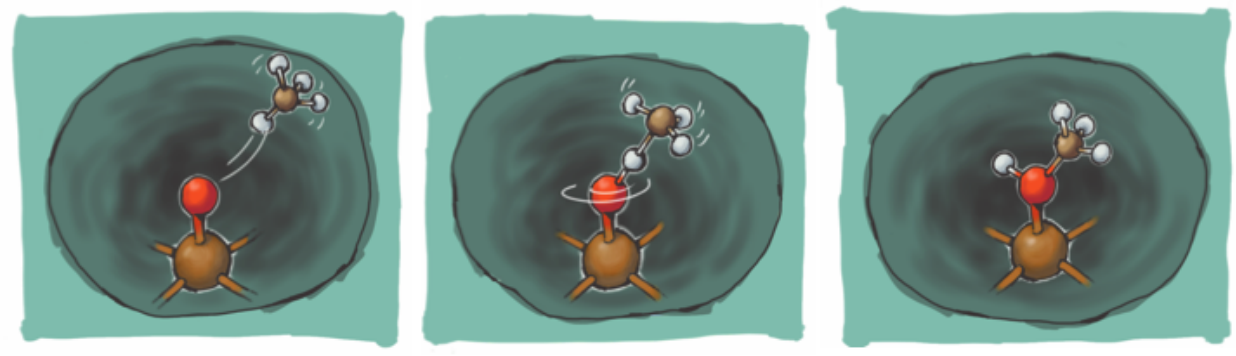

Scheme 1: A schematic representation of the rebound mechanism for the conversion of methane to methanol over Fe-oxo sites. After initial adsorption of the molecule (left), one hydrogen is abstracted before an intermediate (middle) is formed. Methanol (right) is formed after the so called rebound step, where the OH-group rotates around. O atoms are displayed in red, Fe atoms in gold, H atoms in white and C atoms in brown.

For adsorption of methane a straight Fe-O-C angle has been suggested in previous studies in zeolites.[30] However, we find a strongly tilted geometry with an Fe-O-C angle of about 145° (Fig. 1 A) to be more stable. It seems like small differences in van der Waals interactions are decisive in stabilizing the bent configuration. This also holds for the hydrogen abstraction transition state with an angle of 150° (Fig. 1 B). In the intermediate structure the H atom is already clearly bonded to the O atom of the Fe-oxo group and in contrast to the initial tetrahedral C-H angles the resulting methyl group is entirely flat (Fig. 1 C). To form methanol (Fig. 1 E) the OH-group rotates away in the rebound step before the C-O bond can be formed. In this second transition state (Fig. 1 D) the OH-group is rotated by about 70° around the Fe-O axis compared to the case of the intermediate.

If we now turn to the energy profile, for PBE-D2 the highest energetic barrier along this reaction path corresponds to the abstraction of hydrogen with a value of about 25 kJ/mol (see Fig. 2). The intermediate is stabilized by only 7 kJ/mol before another barrier of

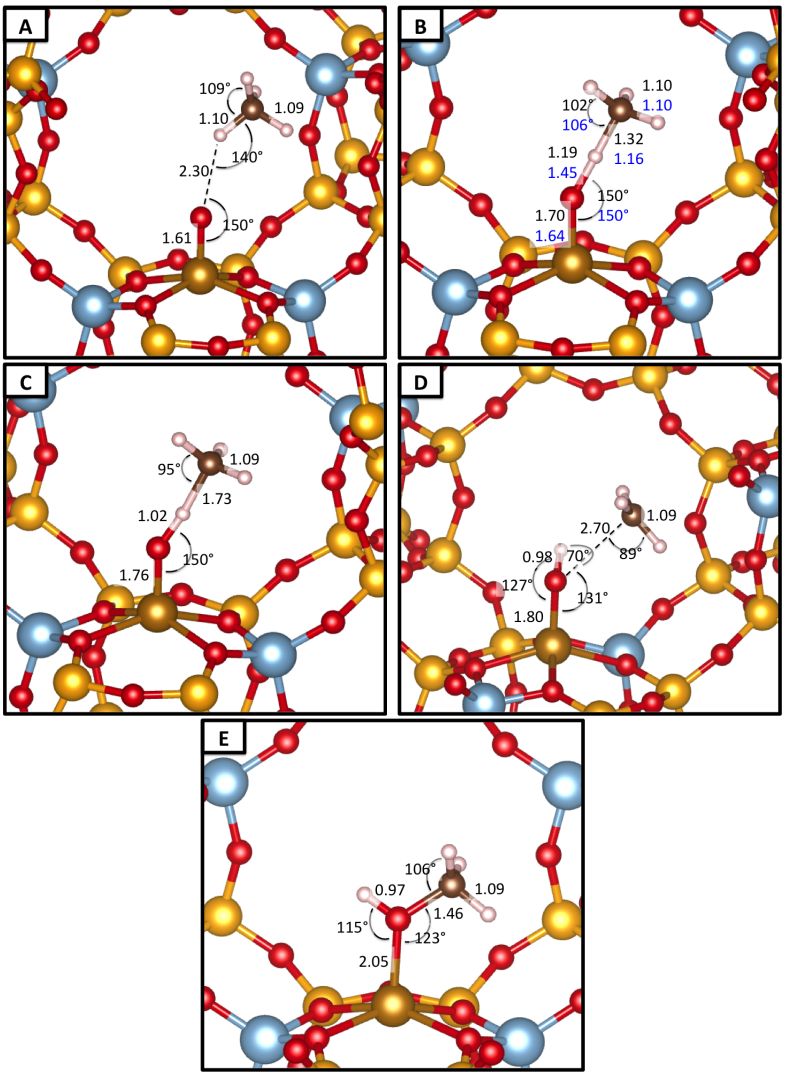

Figure 1: Structures and the most important intermediates (adsorbed molecule (A), reaction intermediate (C) and adsorbed methanol (E)) and transition states (abstraction transition state (B) and rebound transition state (D)) along the reaction pathway. Si atoms are displayed in yellow, O atoms in red, Al atoms in blue-grey, Fe atoms in gold, H atoms in white and C atoms in brown. Black numbers represent PBE-D2 distances (in Å) and angles (in °, blue numbers in B show the optimized RPA geometry.

about 8 kJ/mol needs to be overcome for the second transition state. The total reaction is highly exothermic with an energy gain of more than 150 kJ/mol for the adsorbed methanol compared to the initially adsorbed methane molecule. At this point it is necessary to point out that the effective barrier, combining the first and second TS is 26 kJ/mol.

To calculate RPA energies we rely on PBE-D2 input geometries. However, to arrive at a better guess for the hydrogen abstraction transition state, we performed a nudged elastic band calculation between the initial state and the reaction intermediate at PBE-D2 level and subsequently calculated RPA energies for each of these structures (see Fig. S2 in the Supporting information). This allows a structural optimization along the reaction coordinate, i.e. a change in the C-H-O distances, with the other coordinates still being optimized at GGA-level. In this approach we assume that errors in the other coordinates, caused by using PBE-D2 input geometries, cancel out. With this method we find a significantly earlier transition state for hydrogen abstraction (see Fig. 1 B), even though the barrier is with 24 kJ/mol very similar to that with PBE-D2. However, the energy profile changes dramatically when studying the intermediate, where we find a strong stabilization with RPA, compared to PBE-D2. We then applied to the rebound transition state an approach similar to the one described previously for the hydrogen abstraction transition state, but did not find any structural changes. The energetic barrier is with 3 kJ/mol even smaller than that for PBE-D2. Finally, the stabilization of the adsorbed methanol is with 240 kJ/mol far stronger for RPA than for PBE-D2.

These large differences in the stabilization of the intermediate and final structure are quite concerning and three possible contributions might lead to them: (i) a loss of error cancellation upon the breaking of the C-H and formation of the O-H bond, (ii) intrinsic problems in the description of the chemical activity of the site at PBE level, or (iii) a change of van der Waals interactions due to changes in the polarizability of the Fe-oxo-adsorbate complex induced by a different coordination environment of the given atoms.

While understanding a possible loss in error-cancellation is tricky, due to the complexity

of the potential energy surface, one possible strategy to elucidate the impact of confinement is to find a comparable system where the impact from confinement is eliminated. We follow this strategy by constructing a cluster containing only six T-sites, and the respective OH terminations (displayed on the right hand side of Fig. 2) for all the different structures. This cluster is the smallest one possible that allows a similar chemical environment for the active site compared to the fully periodic framework. To minimize problems with the H-termination we then only optimize the structures of the terminal H-atoms and place this cluster in a 11 Å x 11.5 Å x 13 Å orthorombic unit cell shown on the right hand side in Fig. 2. Careful tests reveal lateral interactions between clusters in different unit cells. We therefore corrected results in an ONIOM type approach[35] with calculations for a cluster in a 20 Å x 20.5 Å x 21 Å orthorombic unit cell at PBE-D2 level. The calculated values for the different unit cell sizes are reported in Table S1 in the Supporting Information.

The energies for both methods change significantly compared to the calculations for the periodic structure (see right hand side of Fig. 2). For the cluster, the activation energy increases to about 60 kJ/mol for both methods, and again, the intermediate is stabilized significantly stronger for RPA than for PBE-D2. However, compared to fully periodic calculations, they are more than 40 kJ/mol higher in energy, a trend that is also seen for the rebound transition state. Interactions between molecule and cavity wall seem to stabilize the intermediate structure significantly stronger than the second transition state, which leads to a lower energy for this TS in the cluster calculations. Again the reaction is highly exothermic, but energies are 60-80 kJ/mol higher than for the periodic structures. These large energetic differences clearly show that confinement effects indeed stabilize the reaction intermediates and products in zeolites by 40-80 kJ/mol and lower the observed effective reaction barriers by more than 50% for the given structures.

In the past, confinement effects have been attributed to electrostatic interactions due to static dipole moments as well as dispersion forces.[13,14] Already when analyzing the energetics at PBE level (i.e. without the -D2 correction, see supporting information Table S2), we find,

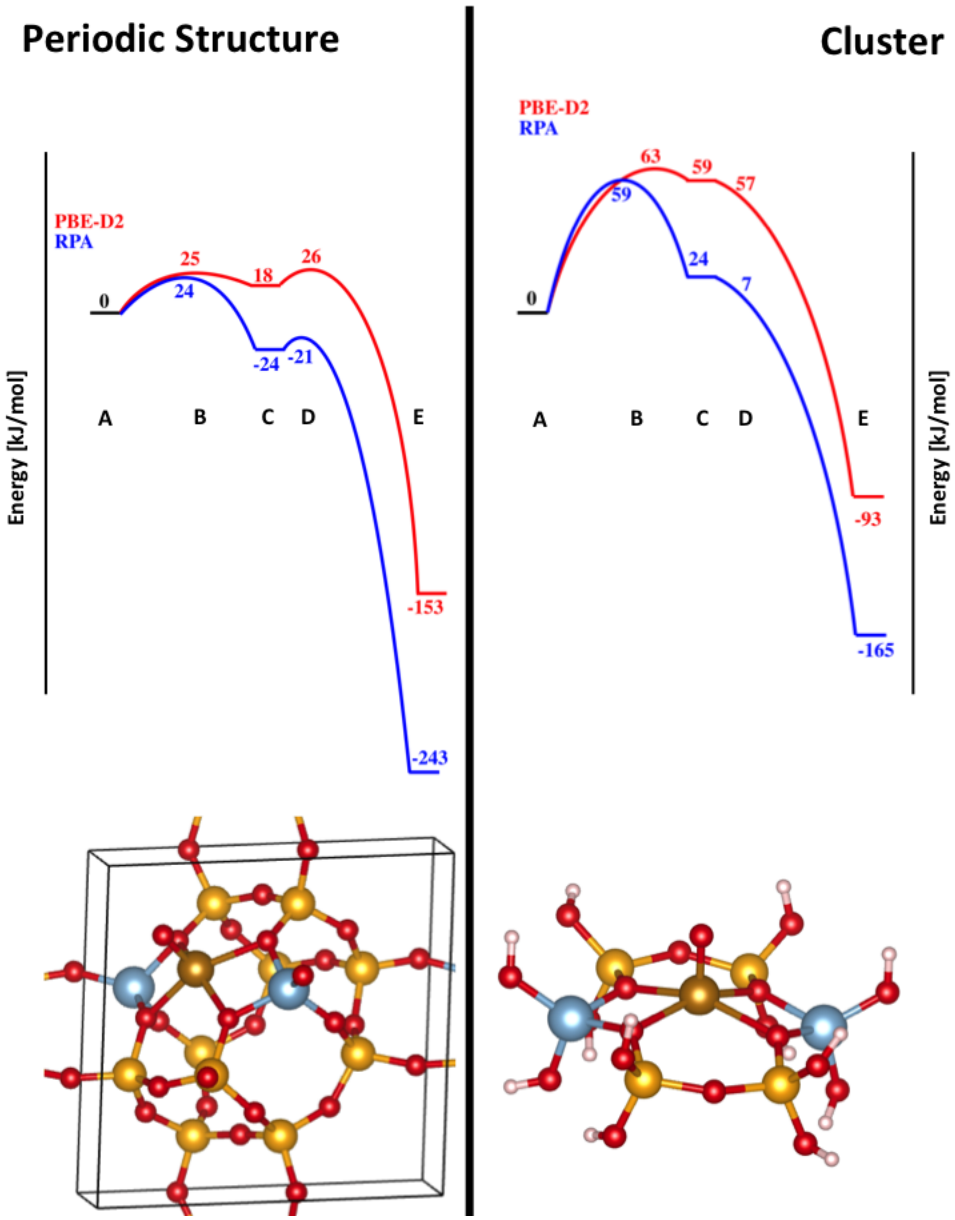

Figure 2: Reaction energetics for the rebound mechanism in methane to methanol conversion calculated at PBE-D2 (red line) and RPA level (blue line) for the periodic structure (left hand side) and a minimal cluster (right hand side). The intermediate structure is stabilized significantly for RPA. For both systems we find a significant stabilization for the transition states, intermediate structure and methanol when moving from PBE-D2 to RPA. Furthermore, the large energy differences between fully periodic and cluster calculations show an important impact of confinement on this reaction. The color code for the structural models and the structures corresponding to A-F are given in Fig. 1.

compared to PBE-D2, similar relative stabilities of the different reaction intermediates and products in periodic calculations and for the cluster models. Combined with a Bader charge analysis, that shows that the charges located at the C and H atoms as well as the Fe-oxo group change significantly along the reaction pathway (see supporting information Figure S3), this indicates that confinement influences the reaction energetics mainly due to changes in electrostatic interactions along the reaction path between the multipole moments of the Fe-oxo-adsorbate complex and the cavity walls.

At the same time the energies are still significantly different between the two methods RPA and PBE-D2 for the cluster model. Since the confining environment has mainly been eliminated in the cluster calculations, a large part of these differences must be related to differences in describing the chemical interactions between the molecule and the active site. Similar conclusions have been reached by Tuma et al., who compared PBE-D2 and MP2 reaction pathways for the deprotonation of tert-butyl to isobutane and its conversion into surface alkoxides.[25] They concluded that it was not possible to capture the full complexity of interactions using an approach as simple as PBE-D2, since it does not include the self-interaction correction. When now comparing fully periodic and cluster calculations we only find minor differences in energy changes for the different applied electronic structure methods, which might be related in the differences in describing van der Waals interactions between them.

At the same time it is important to mention that the barriers for both reaction steps are very similar in both methods, but due to the strong stabilization of the intermediate the rate limiting transition state is shifted. While it is the rebound transition state for PBE-D2, the strong stabilization of the intermediate shifts it to the hydrogen abstraction transition state for RPA. This shift is especially important when considering the impact of confinement on the reaction barriers in this context. Our cluster calculations indicate that electrostatic interactions stabilize the intermediate more than the adsorbate. Therefore, following Brønsted-Evans-Polanyi relationships, in this reaction, a tighter confinement will

lower the activation barriers. This change is significant and our calculations indicate that the presence of confinement lowers the effective barrier of the catalytic reaction by 50%. This has also been observed in the work of Vanelderen et al.,[6] who showed different activation enthalpies for two different active sites in Cu-exchanged Mordenite. Indeed the activation barriers for the more tightly confined site were lower. This could also be due to the differences in adsorption enthalpies. However, comparing these barriers to computational data from Bučko and Hafner[36] for propane and extrapolating it to methane, shows, that the differences in adsorption enthalpies between the narrower 8-ring and wider 12-ring channels are too small to be fully responsible for this effect.

In this work we studied the reaction energy profiles for methane-to-methanol conversion over Fe-oxo sites in the SSZ-13 zeolite at different levels of theory. By comparing calculations for the fully periodic structure to cluster calculations we were able to arrive at three conclusions: (i) in this reaction, confinement stabilizes all transition states, the reaction intermediate and products significantly stronger than the initially adsorbed methane molecule, mainly due to electrostatic effects. (ii) For this reaction, the key effect of confinement is the stabilization of the intermediate. Since it is stabilized more strongly than the initially adsorbed molecule, a more tight confinement will lead to a lower activation energy. (iii) The applied methods lead to significant, qualitative differences in the observed reaction energetics. These differences are mainly due to differences in the description of the chemical bonding. In the future it will be interesting to see how this work can be used to identify more reliable and efficient methods to describe reactions in zeolites. While fully periodic calculations for larger zeolite structures at the RPA level might still be elusive at this point in time, especially hybrid functional calculations are promising candidates to overcome the problems associated with semi-local DFT calculations and might allow to arrive at a qualitatively correct description of reactions in these systems. Additionally further work is needed in the future to see how the 'proof of concept' of the influence of confinement on the methane-to-methanol conversion can be transferred to other zeolite structures to obtain a detailed

understanding of the impact of the pore geometry beyond the system studied in this work.

Computational Setup

All calculations were performed using the Vienna Ab-Initio Simulation Package (VASP),[37,38] a plane wave code using PAW pseudo potentials,[39] adapted by Joubert and Kresse.[40] All calculations were performed using an energy cut-off for plane waves of 600 eV and were restricted to the Γ-point. As mentioned in the main text calculations were carried out using the PBE-D2[26,27] exchange correlation functional and RPA in the implementation discussed by Harl and Kresse.[28] Structures were optimized using PBE-D2 and forces were considered to be converged if they were smaller than 0.02 eV/Å. Reaction intermediates were optimized using a generalized gradient algorithm. Transition states were identified using a combination of the nudged-elastic band climbing-image[41] and dimer methods.[42] For RPA calculations we performed a nudged-elastic band calculation with 16 images spanning from the initial to the intermediate position running through the optimized transition state. In this calculation the spring constant was set to 100 eV/Å^2 to retain a reasonable spacing between the images. After the calculation of the RPA energies for all of the images, we performed a second nudged-elastic band calculation between the neighboring images of the RPA transition state to refine its energetics (images 9-16 in Fig. S2). The cluster models were constructed by keeping the positions of all atoms fixed in the positions of the periodic calculations and only allowing the terminating H atoms to optimize. In the ONIOM-type approach we calculated the total energies as $E^{HL}_{total} = E^{LL}_{small} + E^{HL}_{small} - E^{LL}_{small}$, where X stands for the desired method and small and large denote the unit cell sizes. The basic unit cell parameters for periodic calculations are given in the literature[43] and the volume was set to 830 Å^3.

Supporting information

An analysis of the energies of different spin states, the detailed energetics for the optimization of the hydrogen abstraction step using RPA, energetics for PBE calculated for the fixed PBE-D2 structures and a Bader charge analysis of the different intermediates are provided in the Supporting Information.

Acknowledgements

F. G. and P. S. acknowledge support within the ANR project DYQUMA. F. G. and I. H. acknowledge financial support from the University of Wisconsin Madison and the Wisconsin Alumni Research Foundation (WARF). F.G. and I.H. acknowledge computational time at Phoenix Supercomputer, which is in part supported by National Science Foundation Grant CHE-0840494 and the National Energy Research Scientific Computing Center (NERSC), a DOE Office of Science User Facility supported by the Office of Science of the U.S. Department of Energy under Project No. m2070-Zeo-genome. The authors furthermore acknowledge computational time at the Póle Scientifique de Modélision Numérique (PMSN).

References

(1) Hammond, C.; Conrad, S.; Hermans, I. *ChemSusChem* **2012**, 1668-1686

(2) Leberman, R.L.; Rosenzweig, A.C., *Nature* **2005**, *434*, 177-182

(3) Balasubramanian, R.; Smith, S.M.; Rawat, S.; Yatsunyk, L.A.; Stemmler, T.L., Rosenzweig, A.C.; *Nature* **2010**, *465*, 115-119

(4) Shu, L.; Nesheim, J. C.; Kauffmann, K.; Mnck, E.; Lipscomb, J. D.; Que, L.; *Science* **1997**, *275*, 515-518

(5) Woertink, J.S.; Smeets, P.J.; Groothaert, M.H.; Vance, M.A.; Sels, B.F.; Schoonheydt R.A.; Solomon, E.I *Proc. Nat. Ac. Sci.* **2009**, *106*, 18908-18913

(6) P. Vanelederen, B.E.R. Snyder, M.-L. Tsai, R.G. Hadt, J. Vancauwenbergh, O. Coussens, R.A. Schoonheydt, B.F. Sels, E.I. Solomon, *J. Amer. Chem. Soc.* **2015** *137*, 6383-6392

(7) Wulfers, M.J.; Teketel, S.; Ipek, B.; Lobo, R.F. *Chem. Commun.* **2015**, *51*, 4447-4450

(8) Grundner, S.; Markovits, M.A.C.; Li, G.; Tromp, M.; Pidko, E.A; Jensen, E.J.M.; Jentys, A.; Sanchez-Sanchez, M.; Lercher, J.A.; *Nat. Commun.* **2015**, *6*, 7546

(9) Panov, G.; Sobolev, V.; Dubkov, K.; Parmon, V.; Ovanesyan, N.; Shilov, A.; Shteinman, A.; *React. Kinet. Catal. Lett.* **1997**, *61*, 251-258

(10) Starokon, E.V.; Parfenov, M.V.; Aezumanov, S.S.; Pirutko, L.V.; Stepanov, A.G.; Panov, G.I. *J. Catal.* **2013**, *300*, 47-54

(11) Narsimhan, K.; Iyoki, K.; Dinh, K.; Leshkov-Roman, Y.; *ACS Cent. Sci.* **2016**, *2*, 424-429

(12) Bhan, A.; Iglesia, E.; *Acc. Chem. Res.* **2008**, *41*, 559-567

(13) Gounder, R.; Iglesia, E.; *Acc. Chem. Res.* **2012**, *45*, 229-238

(14) Boronat, M.; Marinez, C.; Corma, A.; *Phys. Chem. Chem. Phys.* **2011**, *13*, 2603-2612

(15) Dusselier, M.; Van Wouwe, P.; Dewaele, A.; Jacobs, P.A.; Sels, B.F. *Science* **2015**, *349*, 78-80

(16) Conrad, S.; Verel, R.; Wolf, P.; Göltl, F.; Hermans, I. *ChemCatChem* **2015**, *7*, 3270-3278

(17) Corma, A. *Chem. Rev.* **1995**, *95*, 559-614

(18) B. Smit, T.L.M. Maesen, *Nature* **2008**, *451*, 671-678

(19) Sastre, G., Corma, A., *J. Mol. Catal. A: Chem.* **2009**, *305*, 3-7

(20) Haag. W.O., Lago, R.M., Weisz, P.B., *Faraday. Disc. Chem. Soc.* **1981**, *72*, 317

(21) Haag, W.O., Dessau, R.M., Lago, R.M., in: *Chemistry of Microporous Materials, Stud. Surf. Sci. Catal. 60* **1991**, 255-265

(22) Gounder, R.; Iglesia, E. *Chem. Commun.* **2013**, *49*, 3491-3509

(23) Göltl, F.; Grüneis, A.; Bučko, T.; Hafner, J. *J. Chem. Phys.* **2012**, *137*, 114111

(24) C. Tuma, T. Kerber, J. Sauer, *Angew. Chem. Int. Ed.* **2010**, *49*, 4678-4680

(25) Perdew J.P., Burke K., Ernzerhof M., *Phys. Rev. Lett.* **1996**, *77*, 3865

(26) Grimme, S.; *J. Comp. Chem.*, **2006**, *27*, 1787-1799

(27) Harl, J.; Kresse, G. *Phys. Rev. B* **2008**, *77*, 045136

(28) Andrikopoulos, P.C.; Sobalik, Z.; Novakova, J.; Sazama, P.; Sklenak, S. *ChemPhysChem* **2013**, *14*, 520-531

(29) Rosa, A.; Ricciardi, G.; Baerends, E.-J. *Inorg. Chem.* **2010**, *49*, 3866-3880

(30) Hirao, H.; Hung, W.K.; Moeljadi, A.M.P.; Bureekaew, S. *ACS Catal.* **2015**, *5*, 3287-3291

(31) Shaik, S.; Cohen, S.; de Visser, S.P.; Sharma, P.K.; Kumar, D.; Kozuch, S.; Ogliaro, F.; Danovich, D.; *Eur. J. Inorg. Chem.*, **2004**, 207-226

(32) Ye, S.; Geng, C.-Y.; Shaik, S.; Neese, F.; *Phys. Chem. Chem. Phys.*, **2013**, 8017-8030

(33) Yoshizawa, K.; Shiota, Y.; Yamabe, T.; *Organometallics*, **1998**, *18*, 2825-2831

(34) Morokuma, K.; *Bull. Korean Chem. Soc.* **2003**, *24*, 797-801

(35) Bučko, T.; Hafner J. *J. Catal.* **2015**, *329*, 32-48

(36) G. Kresse and J. Hafner, *Phys. Rev. B* **1993** *48*, 13115

(37) G. Kresse and J. Furthmüller, *Comput. Mat. Sci.* **1996**, *6*, 15-50

(38) Blöchl P.E. *Phys. Rev. B* **1994**, *50*, 17953

(39) Kresse G.; Joubert, D. *Phys. Rev. B* **1999**, *59*, 1758

(40) Henkelman, G.; Uberuaga, B.P.; Jónsson, H. *J. Chem. Phys.* **2000**, *113*, 9901

(41) Heyden, A.; Bell, A.T.; Keil, F.J. *J. Chem. Phys.* **2005**, *123*, 224101

(42) Göltl, F.; Hafner, J., *J. Chem. Phys.* **136**, 064501 (2012)